HHS Public Access

Author manuscript

Langmuir. Author manuscript; available in PMC 2024 August 08.

Published in final edited form as:

Langmuir. 2023 August 08; 39(31): 10806–10819. doi:10.1021/acs.langmuir.3c00727.

Selective Near-Infrared Blood Detection Driven by Ionic Liquid–Dye–Albumin Nanointeractions

Donovan S. Darlington,
Department of Chemistry and Biochemistry, The University of Mississippi, University, Mississippi 38677, United States

Allison N. Mahurin,
Department of Chemistry and Biochemistry, The University of Mississippi, University, Mississippi 38677, United States

Karina Kapusta,
Department of Chemistry and Physics, Tougaloo College, Tougaloo, Mississippi 39174, United States;

Ember Suh,
Department of Chemistry and Biochemistry, The University of Mississippi, University, Mississippi 38677, United States;

Cameron Smith,
Department of Chemistry and Biochemistry, The University of Mississippi, University, Mississippi 38677, United States;

Ethan Jarrett,
Department of Chemistry and Biochemistry, The University of Mississippi, University, Mississippi 38677,United States;

Claylee M. Chism,
Department of Chemistry and Biochemistry, The University of Mississippi, University, Mississippi 38677, United States

Corresponding Author: Eden E. L. Tanner – Department of Chemistry and Biochemistry, The University of Mississippi, University, Mississippi 38677, United States; Phone: 662-915-1165; eetanner@olemiss.edu.

Author Contributions

E.E.L.T.: Conceptualization, supervision, writing – original draft, writing – review and editing, project administration, funding acquisition, resources; D.S.D.: Conceptualization, supervision, writing – original draft, writing – review and editing, project administration, investigation, formal analysis; A.N.M.: Conceptualization, investigation; K.K.: Conceptualization, methodology, software, formal analysis, investigation, writing – original draft, writing – review and editing, resources; E.S.: Conceptualization, investigation, writing – original draft, writing – review and editing; C.S.: Methodology, validation, writing – review and editing; E.J.: Investigation; C.M.C.: Investigation, writing – review and editing; Z.C.K.: Conceptualization, investigation; W.E.M.: Conceptualization, resources, writing – review and editing; J.H.D.: Conceptualization, resources, writing – review and editing; Y.Z.: Conceptualization, writing – review and editing; N.I.H.: Conceptualization, resources; C.S.K.: Investigation, methodology, writing – original draft, writing – review and editing; R.P.S.: Investigation, methodology, writing – original draft, writing – review and editing; N.C.F.: Methodology, resources, formal analysis, writing – original draft, writing – review and editing.

Supporting Information

The Supporting Information is available free of charge at https://pubs.acs.org/doi/10.1021/acs.langmuir.3c00727.
Nineteen figures of fluorescence emission; Three figures of DLS control samples; Full ^{1}H NMR spectroscopic characterizations, water content, and anion structures of all 17 ILs used in this study (PDF)

Complete contact information is available at: https://pubs.acs.org/10.1021/acs.langmuir.3c00727

The authors declare no competing financial interest.

William E. Meador,
Department of Chemistry and Biochemistry, The University of Mississippi, University, Mississippi 38677, United States;

Zakeyia C. Kelly,
Department of Chemistry and Biochemistry, The University of Mississippi, University, Mississippi 38677, United States

Jared H. Delcamp,
Department of Chemistry and Biochemistry, The University of Mississippi, University, Mississippi 38677, United States; Air Force Research Laboratory, Materials and Manufacturing Directorate (RXNC), Wright-Patterson AFB, Dayton, Ohio 45433, United States; UES, Inc., Dayton, Ohio 45432, United States;

Yongfeng Zhao,
Department of Chemistry, Physics and Atmospheric Sciences, Jackson State University, Jackson, Mississippi 39217, United States;

Nathan I. Hammer,
Department of Chemistry and Biochemistry, The University of Mississippi, University, Mississippi 38677, United States;

Chathuri S. Kariyawasam,
Department of Chemistry, Mississippi State University, Starkville, Mississippi 39762, United States

Radha P. Somarathne,
Department of Chemistry, Mississippi State University, Starkville, Mississippi 39762, United States

Nicholas C. Fitzkee,
Department of Chemistry, Mississippi State University, Starkville, Mississippi 39762, United States;

Eden E. L. Tanner
Department of Chemistry and Biochemistry, The University of Mississippi, University, Mississippi 38677, United States; Phone: 662-915-1165;

Abstract

Due to its abundance in blood, a great deal of research has been undertaken to develop efficient biosensors for serum albumin and provide insight into the interactions that take place between these biosensing molecules and the protein. Near-infrared (NIR, >700 nm) organic dyes have been shown to be effective biosensors of serum albumin, but their effectiveness is diminished in whole blood. Herein, it is shown that an NIR sulfonate indolizine-donor-based squaraine dye, SO_3SQ, can be strengthened as a biosensor of albumin through the addition of biocompatible ionic liquids (ILs). Specifically, the IL choline glycolate (1:1), at a concentration of 160 mM, results in the enhanced fluorescence emission (“switch-on”) of the dye in the presence of blood. The origin of the fluorescence enhancement was investigated via methods, including DLS, ITC, and molecular dynamics. Further, fluorescence measurements were conducted to see the impact

the dye–IL system had on the fluorescence of the tryptophan residue of human serum albumin (HSA), as well as to determine its apparent association constants in relation to albumin. Circular dichroism (CD) spectroscopy was used to provide evidence that the dye–IL system does not alter the secondary structures of albumin or DNA. Our results suggest that the enhanced fluorescence of the dye in the presence of IL and blood is due to diversification of binding sites in albumin, controlled by the interaction of the IL–dye–albumin complex.

Graphical Abstract

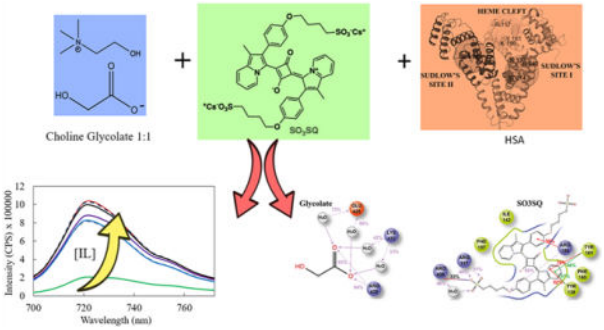

INTRODUCTION

Albumin is the most abundant protein in the blood serum and, therefore, makes an ideal target for sensing blood.[1,2] NIR-emitting dyes are garnering a lot of attention due to their uniquely high emission output, which can be exploited for biosensing and bioimaging.[3,4] Small molecule organic fluorophores that emit in the NIR are advantageous in that they result in increased resolution of internal biological systems due to decreased scattering and absorption of NIR light; some undergo a sharp increase in fluorescence quantum yield (Φ_F) upon an interaction with specific biomolecules and demonstrate biocompatibility with important blood proteins and nucleic acids. Recently, a NIR emissive sulfonate indolizine-donor-based squaraine dye (SO_3SQ) was observed to exhibit a remarkably intense fluorescence quantum yield (Φ_F of 58%) in the presence of fetal bovine serum.[1,2] A further increase in Φ_F to 61.1% was observed when SO_3SQ was dissolved in human serum albumin (HSA).[1,2] An investigation of this phenomenon revealed that the source of the enhancement was the interaction between the dye and the heme cleft site of albumin, where the dye was locked into an “ultrabright” configuration.[2] However, we report herein that SO_3SQ is noticeably less fluorescent in whole blood compared to that in a solution containing pure albumin protein, likely due to the highly complex microenvironment in the blood matrix.

Therefore, we investigated the effect of the addition of biocompatible ionic liquids (ILs) on the selective fluorescence of SO_3SQ in the presence of whole blood. ILs are a class of compounds that are viscous salts at room temperature.[5–7] They consist of asymmetric cations and anions and are extremely tunable for use in a variety of applications, including catalysis, antimicrobials, nucleic acid research, drug delivery, and biosensing.[3–8] In this work, the ILs are being considered as additives rather than solvents, where they interact with SO_3SQ dye and albumin molecules in an aqueous solution. There has been a swath of research conducted on the interaction of ILs with various proteins, including albumin.[7,9–15]

These investigations experimentally examined changes in the protein's structure when interacting with the ILs and utilized Molecular Dynamics (MD) simulations to gain insight into the strength of the IL/albumin interactions.[9–13] It was determined that ILs containing an imidazolium cation caused domain I in HSA to favor a more unfolded state, while the IL containing a cholinium cation allowed HSA to maintain a stability similar to when it is in an aqueous solution.[9,14,15] More recent research involving imidazolium-based ILs and HSA revealed that the percentage of cation binding to the protein was dependent upon the chain length of the imidazolium cation. Therefore, it was hypothesized that tuning the structure of ILs to control and enhance the interaction between the SO_3SQ dye and albumin could result in the switch on/off fluorescence in complex matrices such as whole blood, with a view to developing a sensitive biosensor with a forensic serological application to detect latent bloodstains.

EXPERIMENTAL SECTION

Materials.

Choline bicarbonate (80% in water) and the respective anions used in the IL synthesis are commercially available and purchased from Sigma-Aldrich (Milwaukee, WI) and TCI America (Portland, OR). Lyophilized HSA (96% pure) was purchased from Sigma-Aldrich (Milwaukee, WI). SO_3SQ dye was synthesized as previously described.[3] Human whole blood was purchased from Bio-IVT (Gender pooled, stored cold, and delivered next-day, Westbury, NY) and used as approved by the Institutional Biosafety Committee at the University of Mississippi. A Milli-Q IQ 7000 water purification was used to produce the water (resistivity of 18.2 MΩ·cm at 25 °C) used for sample preparation. Polished quartz cuvettes with a path length of 1 cm were purchased from Hellma Analytics for fluorescence spectroscopy. For light scattering experiments to measure the size of the system, DTS0012 cuvettes were purchased from Sarstedt (Newton, NC) and folded capillary cells for measuring zeta potential were obtained from Malvern Panalytical (Malvern, U.K.).

METHODS

Synthesis and Characterization of ILs.

The ILs are synthesized according to previously published reaction procedures.[10] The ILs are prepared in 1:1 or 1:2 choline/anion ratios via a salt metathesis reaction (Scheme 1). Briefly, the anion is placed in a round-bottomed flask on a hot plate at 50 °C. The choline bicarbonate is then added dropwise. After the addition is complete, the solution is left stirring at 270–300 rpm at a temperature of 50 °C for 24 h. After 24 h, the solution is placed on a rotary evaporator for 1 h at 15 mbar to remove excess water. The IL is then placed in a vacuum oven set to 60 °C and −760 mmHg relative to ambient pressure for 48 h. The water content of the IL is then measured by using a Karl Fischer coulometer (Metrohm). Because we can correct for water content before addition to aqueous solution, achieving ultradry ILs was not necessary. With that said, ILs were dried until they contained less than 10% w/w. Choline glycolate (1:1) was measured as 1.17% water w/w (water content for the rest of the ILs is provided in the SI). The ILs are then characterized via ^1H NMR spectroscopy (as fully detailed in SI).

Conductivity Measurements.

Conductivity was measured using a Thermo Scientific Orion Star A212 conductivity meter using a DuraProbe 4-electrode conductivity cell. The 160 mM solutions of CG 1:1 were prepared in either water or SO3SQ. For the purpose of comparing conductivities, solutions of 160 mM of choline bicarbonate and glycolic acid, as well as NaCl, were also prepared in water and dye. The clean probe was introduced into each solution to record the conductivity. The conductivity was measured in triplicate for each of the solutions.

Fluorescence Measurements of Dye/IL Systems.

A 10 μM SO_3SQ stock solution was prepared in Milli-Q water, and the volume of this solution for each fluorescent measurement was held constant at 3 mL. To record the initial fluorescence intensity of the system without ILs, 0.5 μL of human whole blood was added to the 3 mL of dye solution. To test the impact the ILs had on the dye's fluorescence (both with and without blood), each IL was added in 40 mM increments until a final IL concentration of 240 mM was reached. This resulted in seven different IL concentrations to be tested: 40, 80, 120, 160, 200, and 240 mM. The fluorescence measurements were recorded with an excitation wavelength of 690 nm and emission was monitored from 700–772 nm. The slit widths for excitation were set to 8 nm, and the emission slit widths were set to 15 nm. The steadystate emission data was collected using a Horiba PTI QuantaMaster QM-8075–21 fluorometer (Horiba, Kyoto, Japan) equipped with a silicon-based PhotoMultiplier Tube (PMT) in the visible region (700–772 nm) with a step size of 4 nm and excitation and emission slit widths at 3 and 1.5 nm, respectively, with 690 nm used as the excitation wavelength from a 75 W xenon lamp. For both the neat and IL-addition dyes, Milli-Q water was used as the solvent. Emission blanks of the relevant solvents were subtracted from subsequent dye and IL-addition dye emission. Sample and reference concentration was kept below 1 Abs unit to minimize inner filter effects.[17] Rectangular 10 mm path cuvettes were used for all fluorescence measurements under an ambient atmosphere.

Fluorescence Measurements of Albumin Tryptophan Residue.

Samples were prepared by using a freshly made 10 μM stock solution of SO_3SQ in water. The sample volume for analysis was 3 mL. Lyophilized HSA was added into these samples at 0.1 mg/mL. Control samples were run in Milli-Q water. Twenty-five μL of CG 1:1 was added after each subsequent scan to increase the solution's CG 1:1 concentration by 40 mM upon each addition. The impact of the IL's concentration on the tryptophan residue's fluorescence was done in water both with and without SO_3SQ present. In these samples, the required volume of IL was added to a solution of water and albumin (0.2 mg/mL). Twenty μM SO_3SQ stock solution was added 1:1 with the HSA/water/IL solution to achieve a final dye concentration of 10 μM and to maintain a concentration of 0.1 mg/mL HSA. The fluorescence measurements for all three scans were recorded with an excitation wavelength of 275 nm, and the emission was monitored over the range of 285–415 nm, as described above. Although tryptophan is the dominant emitting species in HSA, it is important to note that fluorescence due to the more abundant tyrosine residues is also present if exciting at a wavelength of 275 nm. To combat this, previous literature states that tryptophan residues can be targeted specifically without exciting tyrosine residues if the excitation wavelength

is around 290–295 nm.[18] These additional measurements were carried out at an excitation wavelength of 295 nm, with emission being monitored over the range of 305–415 nm.

Dynamic Light Scattering (DLS).

DLS size and zeta potential measurements of the systems containing HSA were performed on a Malvern Panalytical Zetasizer Advance Series instrument. All measurements were performed at a constant temperature of 25 °C with water as the dispersant (refractive index, 1.33; viscosity, 0.887 cP; dielectric constant, 78.5). Hydration particle size was measured as intensity. SO_3SQ (10 μM in water) was set as the primary material for each scan, and its refractive index and absorptivity are 0.9 and 1.2, respectively. Samples of HSA were prepared at 0.1 mg/mL of either water or 10 μM SO_3SQ. The IL CG 1:1 was added at 160 mM, the concentration that yielded the maximum fluorescence intensity. The system of HSA in water with and without IL was measured along with the system of HSA in 10 μM SO_3SQ with and without IL. Each sample was prepared fresh three times to allow the size and zeta potential to be measured in triplicate.

Isothermal Titration Calorimetry (ITC).

ITC measurements were carried out in triplicate on a Malvern VP-ITC. Uncertainties are provided as the standard error of the mean. The solvent was either buffer alone (25 mM sodium phosphate, pH 6.5) or buffer plus 40 mM CG 1:1. HSA was dialyzed into the appropriate buffer, and solid SO_3SQ was dissolved in dialysis buffer to ensure a close buffer match. This was necessary in order to prevent strong heats of dilution that are often observed when ILs are titrated in separately. Both HSA and dye solutions were degassed for 10 min before experiments. A typical experiment contained 60 μM HSA in the syringe and 60 μM dye in the calorimetry cell. A total of 28 injections were typically used, each 10 μL in volume, and 10 min of equilibration time was allowed to occur between injections. Measurements were performed at 25 °C. Because injection heats and corresponding signal-to-noise ratios were small, manual baseline fitting was performed using Origin software. Since K and N cannot be determined using this ratio of HSA and dye in the presence of CG 1:1, only the enthalpy is accessible from these measurements. The enthalpy for each ITC experiment was reported as the average enthalpy of the first 10 useable injections, which were all similar. The first injection often exhibited a systematically lower heat than the other injections because of sample diffusion during the experimental setup, and it was not typically used. For reverse titrations, performed without CG 1:1, N, K, and ΔH were fit using CHASM,[19] and the heat of the final injection was used as the baseline. The number of binding sites per HSA molecule was reported as the inverse value of N from fitting, as is typical for reverse titrations.[16] Finally, we also performed titrations where SO_3SQ or HSA was systematically removed, one at a time, in the presence and absence of CG 1:1, to determine whether dilution heats were contributing to the measured enthalpy. In all cases, dilution heats were small, less than 10% of the observed enthalpy, and no further corrections were made.

Circular Dichroism (CD) Spectroscopy.

CD experiments to determine the impact the 1:1 SO_3SQ and CG 1:1 may have on HSA and DNA were performed on a Jasco J-1500 CD spectrophotometer. The measurements were

performed using a Jasco Spectrosil 1 mm path length cuvette. Samples containing HSA were prepared at 1 mg/mL in either water, 10 μM SO_3SQ in water, and 10 μM SO_3SQ in water with 1:1 160 mM CG 1:1 added. The protein scans were conducted at a 200–260 nm range. For measurements involving DNA, bacterial plasmid DNA was used, and the DNA concentration was maintained at 12 nM across all samples due to high instrument sensitivity. CG 1:1 was added at 2.5% v/v to achieve a 160 mM concentration. A solution of 9.14 μM SO_3SQ in water was made and added to DNA solutions in 5 μL increments. These scans were completed over a 200–350 nm range.

Computational Details.

All calculations were performed using the Schrodinger Software Package. The structure of HSA was retrieved from the Protein Data Bank (PDB 1N5U) and prepared by using a Protein Preparation Wizard module. Hydrogen atoms were added, and bond orders were assigned based on their simplified molecular-input, line-entry system (SMILES) strings in the Chemical Component Dictionary (CCD). Missing loops and side chains were filled in using Prime, and the protonation states were generated using Epik with a pH value of 7.0 ± 2.0. The OPLS3e force field was used to optimize the hydrogen bond network and perform restrained minimization. The optimized dye structure was retrieved from our previous work.[4] The 3D structures of choline and glycolate were visualized and subjected to LigPrep. The prediction of the binding pose was achieved with molecular docking and was carried out using the Glide module. Grids were generated being centered on a cocrystallized ligand for the Heme Cleft (*x*: 28.459; *y*: 9.064; *z*: 33.498), important residues of the Sudlow's site I (*x*: 28.424; *y*: 3.344; *z*: 8.941), and the Sudlow's site II (*x*: 3.822; *y*: 2.044; *z*: 22.401) with the length of 40 Å. An extra precision (XP) method and OPLS3e force fields were used for flexible ligand docking. Obtained complexes were further used to refine interactions and estimate binding affinities with the MM-GBSA calculations implemented in Prime. The VSGB solvation model and OPLS3e force field were used. Protein residues at a distance of 12.0 Å from the ligand were set to be flexible. Once the complexes were refined, they were subjected to MD simulations implemented in the Desmond module. Models were built inside the 20.0 Å orthorhombic cell, filled with water molecules (SPC solvent model), and neutralized with Na^+ ions. The temperature and pressure were maintained at 300 K and 1.01325 bar, respectively. The simulation time was set to 50 and 100 ns with a time step of 25 ps. Further, an analysis of trajectories was carried out using the Simulation Interaction Diagram and Trajectory Clustering.

RESULTS AND DISCUSSION

Synthesis and Characterization of ILs.

To test which IL anion generated the largest improvement in the dye's fluorescence in the presence of blood, a large library of choline carboxylate ILs was synthesized using varying anions and characterized as described in the section above. The ILs were synthesized via a salt metathesis reaction (Scheme 1) in which choline bicarbonate and the desired carboxylic acid were combined in 1:1 or 1:2 molar ratios. Several structural features within the ILs were investigated, namely, (1) ratio of choline to anion, (2) chain length, (3) the presence or

absence of double bonds, and (4) the presence of terminal hydroxyl groups. The structures of the anions used can be found in the SI.

Conductivity Measurements.

For the purpose of further comparing the CG 1:1 systems with those containing the IL precursors, conductivity measurements were taken. Previous research has investigated the conductivity of a variety of ILs in aqueous solutions.[20,21] Tsuzuki et al. demonstrate that ILs, despite being ions in solution, show lower conductivity in aqueous solutions due to ion pair formation within the IL.[27] In systems in which ILs are present in aqueous solutions, the conductivity is shown to increase as the solution becomes more and more dilute. This increase in conductivity is attributed to the dissociation of ion pairing caused by the water molecules disrupting the hydrogen bonding between the anion and cation.[20] In the present study of CG 1:1 in aqueous solutions, an average conductivity of 189.4 ± 0.7 μS/cm was measured for the 160 mM CG 1:1 solution in water and an average conductivity of 187.0 ± 0.5 μS/cm for the solution of 160 mM CG 1:1 in SO_3SQ (Table S1 shows all of the conductivity data). At that concentration of IL, this is still a much lower conductivity than that of traditional salts. The solutions of NaCl prepared at a concentration of 160 mM showed an average conductance of 20.4 ± 0.2 mS/cm, 100× higher than that of the IL. Additionally, the IL precursors, choline bicarbonate and glycolic acid, were added into solution, and their conductivity was recorded. For this solution in water, the average conductivity was only 7.0 ± 0.3 μS/cm, while that in SO_3SQ was 13.1 ± 0.1 μS/cm. This data suggest that the IL components are still associated in the aqueous solution as they interact with the SO_3SQ and the albumin.

Fluorescence Measurements.

To assess the ability of each IL to enhance the fluorescence of SO_3SQ dye in human whole blood, the fluorescence emission of 3 mL of a 10 μM dye solution was taken and the fluorescence was measured again after the addition of 0.5 μL of human whole blood. The fluorescence intensity of the dye alone in water shows a 4× increase after the addition of blood (Figure 1C). The addition of blood also results in a redshift of the wavelength of maximum intensity from 716 to 724 nm. From here, fluorescence concentration scans of each IL were performed.

Each IL was scanned from a concentration of 0 to 240 mM and increments of 40 mM were used. The spectra of the concentration scans for each IL can be found in Figures S1–S16. The data obtained from the IL concentration scans confirmed that both the concentrations used and the structural features of each IL anion had an effect on the dye's fluorescence. While some ILs resulted in slight increases in the dye's fluorescence in the presence of blood with increasing concentration, others showed a systematic decrease in the dye's fluorescence in the presence of blood with increasing concentration. ILs of a 1:2 cation to anion ratio resulted in higher fluorescence intensity of the dye in the absence of blood when compared to those of a 1:1 ratio. ILs containing double bonds nearly maintain the dye's maximum fluorescence intensity in the absence of blood, while sharply decreasing it in the presence of blood's presence. Most ILs other than CG 1:1 do not result in a noticeable decrease in the dye's fluorescence intensity in the absence of blood with increasing IL

concentration, perhaps due to the lack of the terminal hydroxyl group that CG 1:1 contains. For dye/IL systems in the presence of blood, no general trends in fluorescence intensity were observed based on alkyl chain length. Since these IL/dye systems are being investigated as a potential alternative bloodstain detection method, there must not be discernible fluorescence in the absence of blood, as this could lead to undesired false positives. Our optimal candidate is therefore an IL that shows both the greatest fluorescence increase in the presence of blood and a suppression of the dye's fluorescence in the absence of blood.

The IL, choline glycolate (1:1) (CG (1:1)), whose fluorescence spectra are shown in Figure 1, was selected as the optimal candidate. The increasing concentration of CG (1:1) showed a noticeable increase in the fluorescence of the dye in the presence of blood (Figure 1A), and a decrease in the fluorescence of the dye in the absence of blood (Figure 1B). To visualize the fold-changes more easily across each system, each figure is normalized relative to the maximum emission intensity of that particular data set. The optimal concentration of CG (1:1) was found to be 160 mM, increasing the dye's fluorescence by a factor of 5 (Figure 1C) in the presence of blood relative to the sample without any IL. To confirm that both the anion and the cation played a crucial role in allowing this fluorescence increase, spectra of 10 μM dye with 160 mM of the IL imidazolium glycolate were also recorded (Figure S17) and showed no appreciable fluorescence enhancement. Additionally, Figure S18 demonstrates that the formation of the IL prior to its addition into the 10 μM aqueous dye solution is of utmost importance, as the glycolic acid or the addition of both choline bicarbonate and glycolic acid together have little impact on the dye's fluorescence after the addition of blood, consistent with the conductivity measurements reported above.

Normalized Fluorescence and System Binding.

With significant increases in the dye's fluorescence being observed due to the presence of 160 mM CG (1:1), the interaction between the dye and IL moieties in the presence of human serum albumin was next explored. Fluorescence intensity of both the 10 μM dye system and the 10 μM dye/160 mM IL system was monitored over a range of albumin concentrations, and a plot was constructed from fitting the data of these normalized fluorescence intensities with the Hill eq (Figure 2). The system containing SO_3SQ and CG is seen to undergo an increase in fluorescence at albumin concentrations lower than those of the system with SO_3SQ alone. An apparent dissociation constant ($K_{D,app}$) and association constant ($K_A = K_{D,app}{}^{-1}$) can be gained from this plot, assuming that all binding sites on HSA are identical and independent, and assuming that binding is saturated. These assumptions may not hold for HSA in the absence of IL, as multiple transitions might be present (Figure 2, black). The $K_{A,app}$ value of HSA in SO_3SQ is estimated to be 3.2×10^5, while the K_A value of HSA in SO_3SQ in the presence of IL is estimated at 9.1×10^5, demonstrating that the IL facilitates greater binding affinity. From the K_A values, the free energy of binding was calculated using this equation: $\Delta G^0_{app} = -RT \ln K_{A,app}$, where R is the gas constant. For the system containing just the dye, the free energy of binding was estimated as −7.4 kcal mol^{-1}, and for the system containing the dye and IL, the free energy of binding was estimated to be −8.0 kcal mol^{-1}. This is consistent with the value previously reported at a concentration of 1 μM.[4] These values show that CG (1:1) allows the dye to bind more favorably to HSA than if the dye is binding HSA by itself.

HSA Tryptophan Fluorescence.

Fluorescence of the tryptophan residue of HSA was measured as a function of increasing IL concentration to provide information about the location of the interaction among SO_3SQ/HSA, CG (1:1)/HSA, and SO_3SQ/CG (1:1). We selected this residue to monitor because the tryptophan residue resides in Sudlow's Site I of HSA,[22] which may be implicated in binding between HSA and the dye.[4] The same IL concentration range was employed here as in the studies monitoring the fluorescence of the dye. To understand whether the order in which the IL or dye is added into the HSA solution has an impact on tryptophan fluorescence, the IL concentration scan was performed under 3 conditions: (1) CG (1:1) added into a solution of 0.1 mg/mL HSA in water (no dye); (2) CG (1:1) added into a solution of 0.1 mg/mL HSA in 10 μM SO_3SQ (dye already present); (3) SO_3SQ added into solutions of 0.1 mg/mL HSA in water with the varying concentrations of CG (1:1; IL already present). Figure 3 shows the resulting tryptophan fluorescence spectra for HSA solutions in the presence of 10 μM SO_3SQ or 160 mM CG (1:1). The spectra of the entire concentration scan for each scenario are shown in Figures S19–S21. Preliminary spectra of tyrosine and tryptophan with excitations at 275 and 295 nm can be found in Figure S22. Adding increasing amounts of CG (1:1) into a solution of HSA in water resulted in a decrease in the intensity of the fluorescence of the tryptophan residue of about 10% (Figure 3B). A 4 nm blueshift from a wavelength maximum of 333 nm to a wavelength maximum of 329 nm was also observed after the addition of CG (1:1). A greater decrease in the intensity of the fluorescence of the tryptophan residues (~70%) was observed in the scenario in which increasing amounts of CG (1:1) were added to a solution of HSA that already contained 10 μM SO_3SQ (Figure 3C, condition 2). For the third scenario, where CG (1:1) was present in the aqueous HSA solution prior to the addition of SO_3SQ, we see the greatest reduction of the fluorescence (~90%, Figure 3D, condition 3). Notably, the change in the concentration of IL after the initial addition did not seem to have an appreciable impact on the tryptophan fluorescence (as distinct from the dye fluorescence reported above, where the optimal concentration was 160 mM). The degree of fluorescent emission correlates with the degree of interaction with the tryptophan residue, with greater decreases indicating a greater interaction. Therefore, we can infer that the IL alone has some interaction with the tryptophan residue in HSA, and this interaction is enhanced greatly in the presence of the dye. The computational details provide the potential mechanism of such an interaction. Interestingly, even greater reductions in the fluorescent emission are observed when the IL is in solution with the HSA as the dye is added, suggesting that the IL may "prime" greater interactions between the albumin and the dye. This will be explored further below.

Computational Modeling.

Previous work investigated the interaction between SO_3SQ dye and HSA.[4] Here the mechanism of tryptophan fluorescence quenching and overall fluorescence increase when the IL is added to the SO_3SQ-HSA complex is investigated. Previous computational modeling revealed the heme cleft being the most favorable binding site with the dye. Additionally, it was shown that the dye's binding into Sudlow's sites I and II was possible after the saturation of the heme cleft, as suggested by the normalized plot of fluorescence intensity versus protein concentration. Hence for this work, all three binding sites are considered. Since ionic liquid components are relatively small compared to the HSA protein,

they can bind to other binding sites of the HSA (fatty acid binding sites). However, only the above-mentioned drugbinding sites are considered for the model's simplicity.

First, both the dye and the IL components were docked to HSA separately. Complexes obtained using molecular docking and MM/GBSA calculations were further subjected to MD simulation. During the 50 ns simulation, SO_3SQ bound to the heme cleft (Figure 4a), and Sudlow's site I (Figure 4b) retained the most significant number of interactions with the protein. When bound inside Sudlow's site I, SO_3SQ formed a hydrogen bond and π–π and π–cation interactions with the tryptophan residue lasting about half of the simulation time. This binding could be a cause for the intrinsic fluorescence quenching of tryptophan residue within the protein, shown in the previous subsection. Even though more hydrogen bonds were formed for the case of Sudlow's site I, the complex of dye with the heme cleft showed an overall better binding pattern with more π–π and π–cation interactions and a more defined shape complementarity, sitting tighter inside of the binding pocket. Inside Sudlow's site II, the ligand was stabilized by only five H-bonds and exhibited a high level of solvent exposure (Figure 4c). MD trajectories were further clustered, and the most populated cluster was used to repeat MM/GBSA calculations for more accurate free binding energy prediction (Figure 4e). Refining of the dye's binding energy showed more negative binding energy when inside of the heme cleft (−108.18 kcal/mol), followed by Sudlow's site I (−69.05 kcal/mol) and Sudlow's site II (−64.04 kcal/mol).

Molecular docking and MM/GBSA calculations demonstrated that the choline cation was a more potent binder for HSA compared to the glycolate anion with an average binding affinity toward all three binding sites of −28.45 kcal/mol (compared to −13.33 kcal/mol in the case of the glycolate). Further, a molecular dynamics simulation demonstrated that within 50 ns of a simulation time, choline left the binding pocket of the protein, unable to form any strong interactions. It is expected that MM/GBSA overestimates the binding affinity. In some cases, only a MD simulation can reveal whether the ligand can actually bind the protein, as was shown for the case study of cannabidiol interacting with CBR1.[23] Considering the results of molecular dynamics, it is concluded that the anion of the ionic liquid (rather than the cation) plays a more important role in interacting with albumin, although the identity of the cation is still crucial (see Figure S17). This conclusion is supported by previously published works.[24] Initially, glycolate bound the strongest within the heme cleft (Figure 4a), forming two H-bonds with R428 (93–94% of a simulation time) and four water bridges with E425 and K432. Docked into Sudlow's sites I and II (Figure 4b,c), it retained H-bonds with K199 and R410, respectively, for about half of the simulation time. In both cases, closer to the end of the simulation time, glycolate migrated toward subunit IIIA (near Sudlow's site II) and bound to R484 and R485. Taking this into account, the last frames of trajectories were used for an additional 50 ns of MD simulations. Migrating from Sudlow's site I, after 22 ns of simulations, glycolate settled near residues R484 and R485. The ligands' RMSD aligned on protein did not exceed 1 Å. Glycolate formed strong H-bonds with R484, R485, and L481, sitting tightly within the positively charged pocket of the protein. The refined free binding energy for this binding site was −22.06 kcal/mol, exceeding the one predicted for the heme cleft. Overall, the strength of binding decreases in a row: a site near R485 > heme cleft > Sudlow's site II > Sudlow's site I (Figure 4e).

The binding of a dye or ionic liquid could indirectly influence the fluorescence of the tryptophan residue, triggering a quenching due to local changes near the interaction site or binding-induced conformational changes. Complexes of SO_3SQ-HSA and G-HSA, obtained by MD simulation followed by clustering and structure refinement with MM/GBSA, were aligned on the original protein structure. Deviations for these complexes varied from 2.5 to 3.5 Å and predominated in subunits IA and IB (Figure 5), which should not influence the properties of only one HSA's tryptophan residue (W214). However, when glycolate was bound in the IIIA subunit near residue R485, a noticeable change in the W214 position was observed (Figure 5b). Thus, the quenching could presumably arise not only from the binding of a dye directly to W214 but also from a conformational change caused by association of HSA with ionic liquid. That explains the decrease in tryptophan fluorescence when ionic liquid was added to the albumin without the dye (Figure 3C).

Further, SO_3SQ-HSA and G-HSA complexes were used to mimic two scenarios used in fluorescence spectroscopy of the tryptophan residue of HSA. The first scenario simulated a case when SO_3SQ is already bound to albumin prior to the addition of IL (Figure 3C), and the second one simulated a case when IL is added first, followed by the addition of SO_3SQ (Figure 3D). For the six complexes of SO_3SQ and glycolate bound to three possible binding sites of HSA, a consequent binding of a dye or ionic liquid to three binding sites was simulated using molecular docking and MM/GBSA (Table 1). In the first scenario, when the dye is already associated with albumin, the affinity for the consequent binding of glycolate to the heme cleft increased (compared to the original −14.78 kcal/mol). In contrast, its binding to Sudlow's site I became less favorable (compared to the original −12.03 kcal/mol). Docking of glycolate into Sudlow's site II showed a noticeable increase in affinity toward HSA when SO_3SQ was in the heme cleft and did not change significantly for SO_3SQ complex bound to other binding sites. The second scenario showed considerably more complex trends. The binding of a dye into the heme cleft of the G-HSA complex was less favorable than its association with unbound HSA. SO_3SQ docked into Sudlow's site I showed increased affinity only when glycolate was present in Sudlow's site II. The presence of glycolate in subunit IIIA near residues R484 and R485 appeared to decrease the overall binding affinity of a dye. The critical change in affinity was noticed for the dye binding into Sudlow's site II of HSA with glycolate in its heme cleft (an increase from −64.04 to −105.34 kcal/mol). Dye's binding to Sudlow's site II was also increased by prior binding of glycolate to the same site. This implies that the presence of ionic liquid could improve the binding of SO_3SQ to Sudlow's site II, thus, increasing the overall binding affinity in a dye–HSA complex.

To test this presumption, a molecular dynamic simulation was carried out for SO_3SQ–IL–HSA complexes, intending to evaluate its stability. First, an increase in the affinity of the dye toward Sudlow's site II of albumin in the presence of an ionic liquid was investigated. The complex with the highest affinity with glycolate being bound in heme cleft and SO_3SQ was in Sudlow's site II and was subjected to a 100 ns MD simulation. At the beginning of the trajectory, a slight rearrangement of the glycolate position was observed. It migrated from the heme cleft to the IIIA subunit and further stabilized in it. Due to this rearrangement, it was more informative to analyze the last half of the trajectory when ligands have already settled. When comparing interactions formed by the dye in the absence of ionic liquid

(Figure 4c) and in its presence (Figure 6a), the binding was more favorable in the latter case. Facilitated by the ionic liquid, SO_3SQ formed an overall larger number of H-bonds and an additional salt bridge with K414, and was less exposed to the solvent with one of the indolizine donors sitting tighter inside of the binding pocket of the protein. That could be caused by conformational changes in subunit III. Thus, one can presume that when an ionic liquid is added to the SO_3SQ–albumin solution, it enables the dye's attachment to binding sites that previously were not as favorable without an ionic liquid. Further, we wanted to verify whether the presence of glycolate in Sudlow's site II may cause a decrease in the binding affinity of the dye for the heme cleft. Like the previous simulation, at the beginning of the trajectory, glycolate migrated from the original binding pocket (Figure 6b). By the second half of the trajectory, it bound to R485. Interactions of SO_3SQ with the albumin's heme cleft did not change significantly, except for the slight overall improvement, fewer π–cation interactions, and the larger number of H-bonds.

Dynamic Light Scattering (DLS).

To further explore the potential formation of HSA–dye–IL complexes, we conducted dynamic light scattering (DLS) measurements were conducted. DLS measurements of the HSA systems with and without IL, either in water or 10 μM SO_3SQ, revealed the formation of complexes and aggregation. Controls of the SO_3SQ dye by itself, CG 1:1 by itself, and SO_3SQ with CG 1:1 in the absence of albumin were also measured with DLS (Figures S20–S22). In the system consisting of HSA in water, light scattering shows a bimodal distribution consisting of smaller complexes (~8 nm) and larger aggregates (~150 nm). When 160 mM 1:1 CG is added, it is incorporated into the HSA complex, as is evident by the sharp increase in the average size. CG 1:1 continues to form its own complexes in solution, which is shown by the sharper peak at ~600 nm (Figure 7A). The average size of the complex increases from 50 ± 30 nm to 430 ± 150 nm, although as can be seen in Figure 7, the distribution is bimodal. The zeta potential data of the system of HSA in water shows that the overall charge of the complex becomes slightly more positive upon the addition of IL, due to the stronger attraction of the cholinium cation of CG 1:1 to the outside of the complex, with its anion counterpart likely burrowed further in to the protein, as indicated by the tryptophan fluorescence and MD simulations in the previous sections (Figure 7B). The average charge is −9.8 ± 0.7 mV prior to the addition of the IL, while the IL increases the average charge of the overall system to −0.17 ± 0.17 mV.

For the system containing HSA in 10 μM SO_3SQ, the addition of 1:1 CG causes the HSA complex (at ~8 nm) to decrease in size slightly while causing a significant increase in the size of the dye complex (~100 nm) (Figure 7C). Overall, the system as a whole shows a slight increase in average size upon the addition of CG 1:1, from 150 ± 20 nm to 170 ± 40 nm. When examining the zeta potential data, an overall increase in the average charge from −20 ± 5 mV to −0.30 ± 0.60 mV is seen due to the fact the IL is rearranging the dye/HSA complex in a way that leads to exposure of the choline cation (Figure 7D).

Isothermal Titration Calorimetry.

Isothermal titration calorimetry (ITC) was utilized next to further characterize the binding. Ionic liquids exhibit strong nonideality, and because of this, they produce significant heats

of dilution in ITC measurements. A careful match between the syringe and the sample cell is needed to eliminate this effect. In this case, SO_3SQ also has limited aqueous solubility (~60 μM), which limits the range of concentrations over which ITC can be performed. Low concentrations of dye are required, which reduces the detectable heat and affects the Wiseman c value.[25] Here, we used substoichiometric concentrations of HSA, titrated into (SO_3SQ) in a reverse titration.[16,26] Under these conditions, ΔH of binding is accessible, but K and N are not.[19] We found that the enthalpy of binding between HSA and SO_3SQ was positive, $\Delta H = 6.1 \pm 0.2$ kcal/mol in a buffer containing 40 mM ionic liquid. Interestingly, the behavior was different in the absence of 1:1 CG 1:1. A complete titration was observable in the reverse experiment, this time with an exothermic heat of binding ($\Delta H = -18 \pm 2$ kcal mol^{-1}, $K = (1.8 \pm 0.4) \times 10^6$, $\Delta G° = -8.50 \pm 0.13$ kcal mol^{-1}, $N = 11.5 \pm 0.4$; uncertainties are standard errors of the mean for three independent trials (Figure 8)). The positive sign of the enthalpy in the presence of an ionic liquid indicates that binding is entropically driven, which would be expected for a hydrophobic dye binding into a pocket on HSA, where binding is driven by the hydrophobic effect. Such entropy-driven binding to HSA has been observed for methylimidazole and amoxicillin binding.[27,28] The fact that the enthalpy is exothermic in the absence of an ionic liquid suggests that the ionic liquid changes the behavior of the solvent, altering the mode of SO_3SQ binding. Work is ongoing to determine a more complete structural and thermodynamic characterization of the binding of SO_3SQ to HSA.

Circular Dichroism (CD) Spectroscopy.

Finally, circular dichroism (CD) spectroscopy was used to test any impact this system may have on the secondary structures of HSA and DNA. When looking at the effect the dye and IL have on HSA (Figure 9A), an increase in the alpha helical content of albumin is observed in a solution of 10 μM SO_3SQ, as well as in a solution of 10 μM SO_3SQ and 160 mM CG (1:1). This increase in the alpha helical content is a result of the initial binding of the protein as it is exposed to these systems; however, its secondary structure is still maintained. CD spectra were also obtained after exposing bacterial plasmid DNA to the test system (Figure 9B). When the DNA is in 2.5% IL solution, the characteristic peaks of the synthetic plasmid DNA are still present at 245 and 265 nm, indicating limited structural changes to the DNA in the presence of the IL (Figure 9B). Before the addition of plasmid DNA, no significant peaks are observed in the CD spectrum of 9.14 μM SO_3SQ dye in water (Figure 9C). However, an apparent minimum peak at approximately 225 nm corresponding to the IL is observed in the CD spectrum of the SO_3SQ dye in a 2.5% IL solution (Figure 9C). After 5 μL of 1 μM dye solution was added for a total of three times to DNA in 2.5% IL (Figure 9D), no significant changes in the CD spectra were seen after each 5 μL addition. Notably, the peaks at 245 and 265 nm, both corresponding to the plasmid DNA's structure, indicate that the SO_3SQ/CG (1:1) causes limited or no structural changes to the DNA. The system's compatibility with albumin and DNA will allow samples that are subjected to it to undergo further protein analysis. This is desirable for future potential application to crime scene investigation, where the DNA obtained from a crime scene is likely to provide the most valuable information. Therefore, this test system must interact with albumin but also not interfere with the structure of DNA.

CONCLUSIONS

Herein it has been determined that it is possible to manipulate the nanointeractions of a NIR dye and albumin through the addition of an IL to control its switch-on fluorescence in whole blood. Specifically, 160 mM of IL CG 1:1 resulted in a 5-fold "switch-on" increase in the SO_3SQ dye's fluorescence in the presence of blood, while suppressing the emission in the absence of blood. Through analysis of the dye's fluorescence in the presence of albumin with and without IL, it was determined that the SO_3SQ/HSA system with 160 mM CG 1:1 had a higher apparent binding association constant ($K_{A,app} = 1.4 \times 10^6$) than the system of just SO_3SQ/HSA (2.0×10^5), thus lending to a more favored free energy of binding for the system with IL. Fluorescence spectroscopy was also used to monitor interactions with the tryptophan residue in the albumin in the presence of dye and/or IL, and we found a decrease in the emission, suggesting an interaction between the IL, dye, and HSA. MD simulations suggest that the IL facilitates additional binding sites in the albumin, resulting in stronger interactions dominated by hydrogen bonding between the glycolate and the albumin. These simulations are supported by ITC measurements, which indicate a balance between entropic and enthalpic effects that can be modulated by the presence of CG. DLS data obtained for HSA in the presence of dye and/or ILs show an increase in both size and charge when IL is added, suggesting the formation of complexes. CD spectroscopy shows that the dye/IL system does not alter the secondary structures of either HSA or DNA, evidencing compatibility for potential further processing. This system therefore shows promise for the future development as a forensic stain, where high sensitivity to blood is paramount.

Supplementary Material

Refer to Web version on PubMed Central for supplementary material.

ACKNOWLEDGMENTS

We thank Susan D. Pedigo for her assistance with CD measurements. E.E.L.T. acknowledges the College of Liberal Arts at the University of Mississippi for funding. E.E.L.T., J.H.D., K.K., and N.H. acknowledge NSF Award 1757220. E.S. acknowledges the Ronald E. McNair Post-Baccalaureate Achievement Program. This material is based upon work supported by the National Science Foundation Graduate Research Fellowship Program awarded to WEM. N.C.F. acknowledges funding from the National Institute of Allergy and Infectious Diseases of the National Institutes of Health under Grant Number R01AI139479 and the National Science Foundation under Grant Number MCB 1818090. The content is solely the responsibility of the authors and does not necessarily represent the official views of the National Institutes of Health or the National Science Foundation.

REFERENCES

(1). Meador WE; Autry SA; Bessetti RN; Gayton JN; Flynt AS; Hammer NI; Delcamp JH Water-Soluble NIR Absorbing and Emitting Indolizine Cyanine and Indolizine Squaraine Dyes for Biological Imaging. J. Org. Chem 2020, 85 (6), 4089–4095. [PubMed: 32037825]

(2). Meador WE; Kapusta K; Owolabi I; Autry SA; Saloni J; Kolodziejczyk W; Hammer NI; Flynt AS; Hill GA; Delcamp JH Ultra-Bright Near-Infrared Sulfonate-Indolizine Cyanine- and Squaraine-Albumin Chaperones: Record Quantum Yields and Applications. ChemPhotoChem 2022, 6 (9), na DOI: 10.1002/cptc.202200127.

(3). Chandran A; Ghoshdastidar D; Senapati S Groove Binding Mechanism of Ionic Liquids: A Key Factor in Long-Term Stability of DNA in Hydrated Ionic Liquids? J. Am. Chem. Soc 2012, 134 (50), 20330–20339. [PubMed: 23181803]

(4). Egorova KS; Posvyatenko A. v.; Larin SS; Ananikov VP Ionic Liquids: Prospects for Nucleic Acid Handling and Delivery. Nucleic Acids Res. 2021, 49, 1201–1234. [PubMed: 33476366]

(5). Figueiredo AM; Sardinha J; Moore GR; Cabrita EJ Protein Destabilisation in Ionic Liquids: The Role of Preferential Interactions in Denaturation. Phys. Chem. Chem. Phys 2013, 15 (45), 19632–19643. [PubMed: 24132185]

(6). Shukla SK; Mikkola JP Use of Ionic Liquids in Protein and DNA Chemistry. Frontiers in Chemistry 2020, 8, na. [PubMed: 32039163]

(7). Singh T; Bharmoria P; Morikawa MA; Kimizuka N; Kumar A Ionic Liquids Induced Structural Changes of Bovine Serum Albumin in Aqueous Media: A Detailed Physicochemical and Spectroscopic Study. J. Phys. Chem. B 2012, 116 (39), 11924–11935. [PubMed: 22954037]

(8). Chism CM; Plash S; Zuckerman D; Dasanayake GS; Bennett M; Tripathi SK; Pedigo SD; Tanner EEL Antimicrobial Effects of Anion Manipulation with Biocompatible Choline Carboxylic Acid-Based Ionic Liquids. ACS Applied Engineering Materials 2023, 1, 23.

(9). Shu Y; Liu M; Chen S; Chen X; Wang J New Insight into Molecular Interactions of Imidazolium Ionic Liquids with Bovine Serum Albumin. J. Phys. Chem. B 2011, 115 (42), 12306–12314. [PubMed: 21919506]

(10). Jaeger VW; Pfaendtner J Destabilization of Human Serum Albumin by Ionic Liquids Studied Using Enhanced Molecular Dynamics Simulations. J. Phys. Chem. B 2016, 120 (47), 12079–12087. [PubMed: 27809527]

(11). Sindhu A; Bhakuni K; Sankaranarayanan K; Venkatesu P Implications of Imidazolium-Based Ionic Liquids as Refolding Additives for Urea-Induced Denatured Serum Albumins. ACS Sustain Chem. Eng 2020, 8 (1), 604–612.

(12). Reddy RR; Shanmugam G; Madhan B; Phani Kumar BVN Selective Binding and Dynamics of Imidazole Alkyl Sulfate Ionic Liquids with Human Serum Albumin and Collagen-a Detailed NMR Investigation. Phys. Chem. Chem. Phys 2018, 20 (14), 9256–9268. [PubMed: 29560969]

(13). Singh G; Kaur M; Kang TS; Aswal VK Aqueous Colloidal Systems of Bovine Serum Albumin and Functionalized Surface Active Ionic Liquids for Material Transport. RSC Adv. 2020, 10 (12), 7073–7082. [PubMed: 35493898]

(14). Kowalska D; Stolte S; Wyrzykowski D; Stepnowski P; Dołżonek J Interaction of Ionic Liquids with Human Serum Albumin in the View of Bioconcentration: A Preliminary Study. Chemical Papers 2022, 76 (4), 2405–2417.

(15). Kumar S; Kukutla P; Devunuri N; Venkatesu P How Does Cholinium Cation Surpass Tetraethylammonium Cation in Amino Acid-Based Ionic Liquids for Thermal and Structural Stability of Serum Albumins? Int. J. Biol. Macromol 2020, 148, 615–626. [PubMed: 31954128]

(16). Le VH; Buscaglia R; Chaires JB; Lewis EA Modeling Complex Equilibria in Isothermal Titration Calorimetry Experiments: Thermodynamic Parameters Estimation for a Three-Binding-Site Model. Anal. Biochem 2013, 434 (2), 233–241. [PubMed: 23262283]

(17). Levitus M Tutorial: measurement of fluorescence spectra and determination of relative fluorescence quantum yields of transparent samples. Methods Appl. Fluoresc 2020, 8 (3), 033001. [PubMed: 32150732]

(18). Burstein EA; Vedenkina NS; Ivkova MN FLUORESCENCE AND THE LOCATION OF TRYPTOPHAN RESIDUES IN PROTEIN MOLECULES. Photochem. Photobiol 1973, 18, 263–279. [PubMed: 4583619]

(19). Lewis EA; Murphy KP Isothermal Titration Calorimetry. Methods Mol. Biol 2005, 305, 1–16. [PubMed: 15939991]

(20). Tanner E; Piston K; Ma H; Ibsen K; Nangia S; Mitragotri S The Influence of Water on Choline-Based Ionic Liquids. ACS Biomaterials Science and Engineering 2019, 5 (7), 3645–3653. [PubMed: 33405745]

(21). Tsuzuki S; Tokuda H; Hayamizu K; Watanabe M Magnitude and Directionality of Interaction in Ion Pairs of Ionic Liquids. Relationship with Ionic Conductivity. J. Phys. Chem. B 2005, 109 (34), 16474–16481. [PubMed: 16853095]

(22). Belatik A; Hotchandani S; Carpentier R; Tajmir-Riahi HA Locating the binding sites of Pb(II) ion with human and bovine serum albumins. PLoS One. 2012, 7 (5), e36723. [PubMed: 22574219]

(23). Wang X; Guo T; Shu Y; Wang J The Anion of Choline-based Ionic Liquids Tailored Interactions Between Ionic Liquids and Bovine Serum Albumin, MCF-7 Cells, and Bacteria. Colloids and Surfaces B: Bio interfaces 2021, 206, 111971.

(24). Akdogan Y; Junk MJN; Hinderberger D Effect of Ionic Liquids on the Solution Structure of Human Serum Albumin. Biomacromolecules 2011, 12 (4), 1072–1079. [PubMed: 21332184]

(25). Wiseman T; Williston S; Brandts JF; Lin L-N Rapid Measurement of Binding Constants and Heats of Binding Using a New Titration Calorimeter. Anal. Biochem 1989, 179, 131. [PubMed: 2757186]

(26). Velazquez-Campoy A; Freire E Isothermal Titration Calorimetry to Determine Association Constants for High-Affinity Ligands. Nature Protocols 2006 1:1 2006, 1 (1), 186–191. [PubMed: 17406231]

(27). Afrin S; Riyazuddeen; Rabbani G; Khan RH Spectroscopic and Calorimetric Studies of Interaction of Methimazole with Human Serum Albumin. J. Lumin 2014, 151, 219–223.

(28). Yasmeen S; Riyazuddeen; Rabbani G Calorimetric and Spectroscopic Binding Studies of Amoxicillin with Human Serum Albumin. Journal of Thermal Analysis and Calorimetry 2016 127:2 2017, 127 (2), 1445–1455.

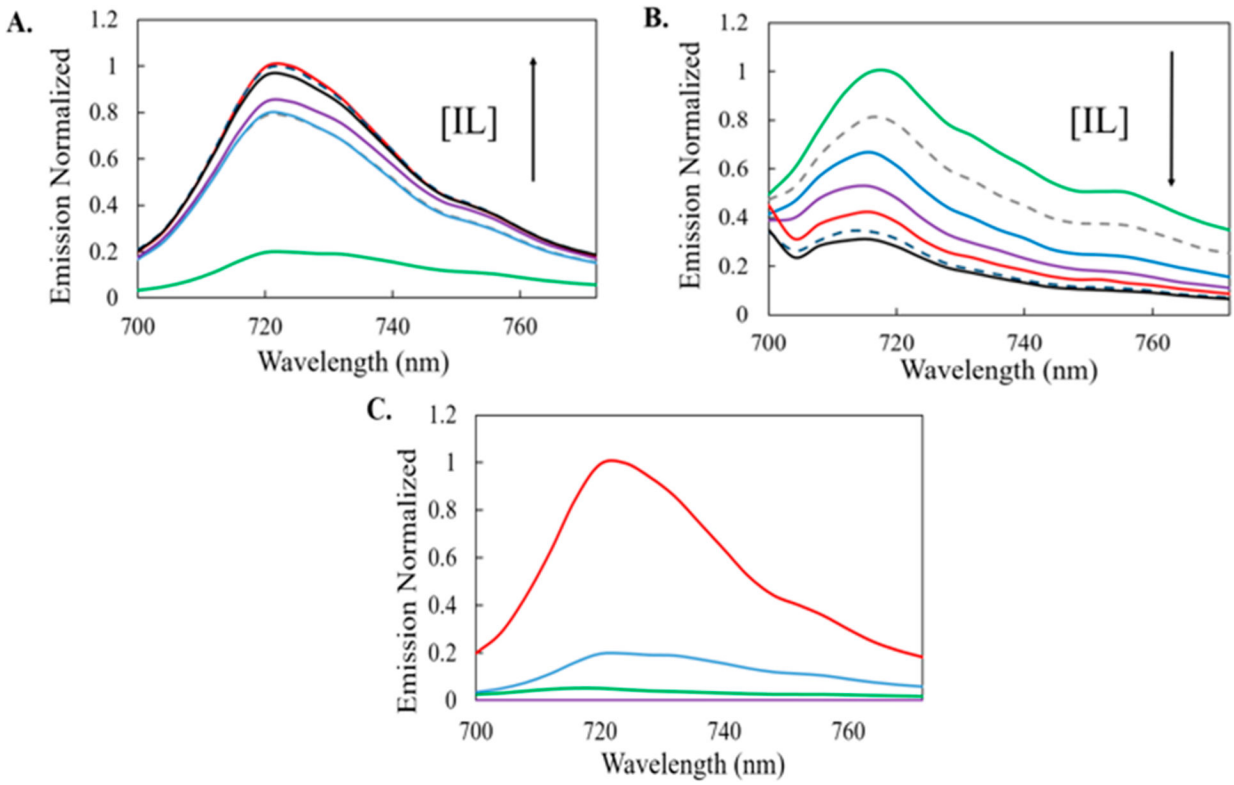

Figure 1.

SO_3SQ dye shows switch-on fluorescence in the presence of blood that is enhanced 5-fold in the presence of 160 mM IL. Fluorescence scans of 10 μM dye in the (A) presence of blood and (B) absence of blood as the concentration of IL is varied from 0 (green solid line), 40 (gray dashed line), 80 (blue solid line), 120 (purple solid line), 160 (red solid line), 200 (navy dashed line), and 240 mM (black solid line) of IL in water. (C) The fluorescent emission of 10 μM SO_3SQ (no IL) in the absence (green line) and presence of blood (blue line) contrasts with the emission in the presence of 160 mM IL in the absence (purple) and presence (red line) of blood.

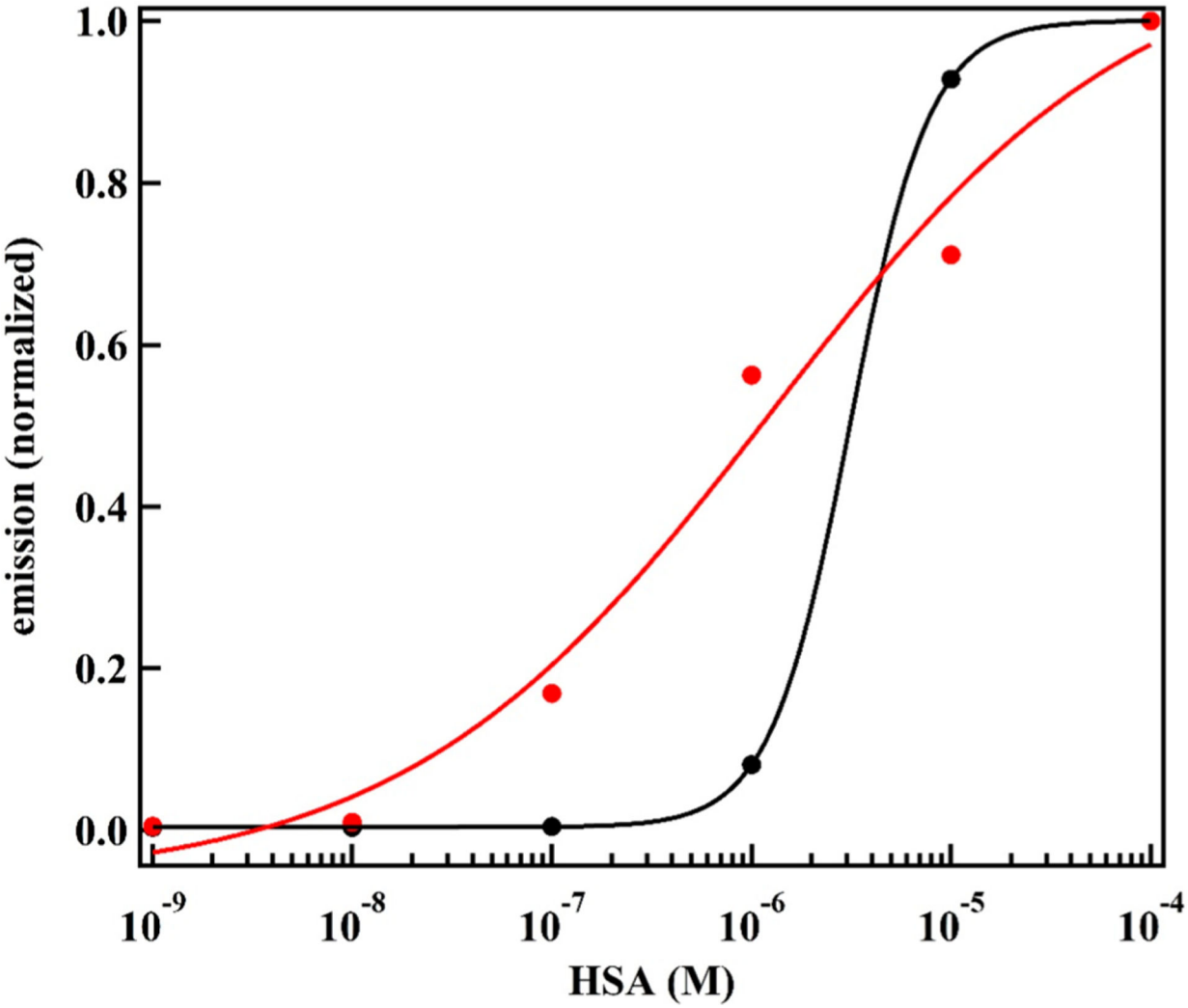

Figure 2.

CG (160 mM, 1:1) allows for a greater binding affinity between SO_3SQ and HSA. Normalized fluorescence intensity as a function of albumin concentration was used to compare the binding affinities of a solution of 10 μM SO_3SQ (black) and a solution of 160 mM CG (1:1) in 10 μM SO_3SQ to HSA (red).

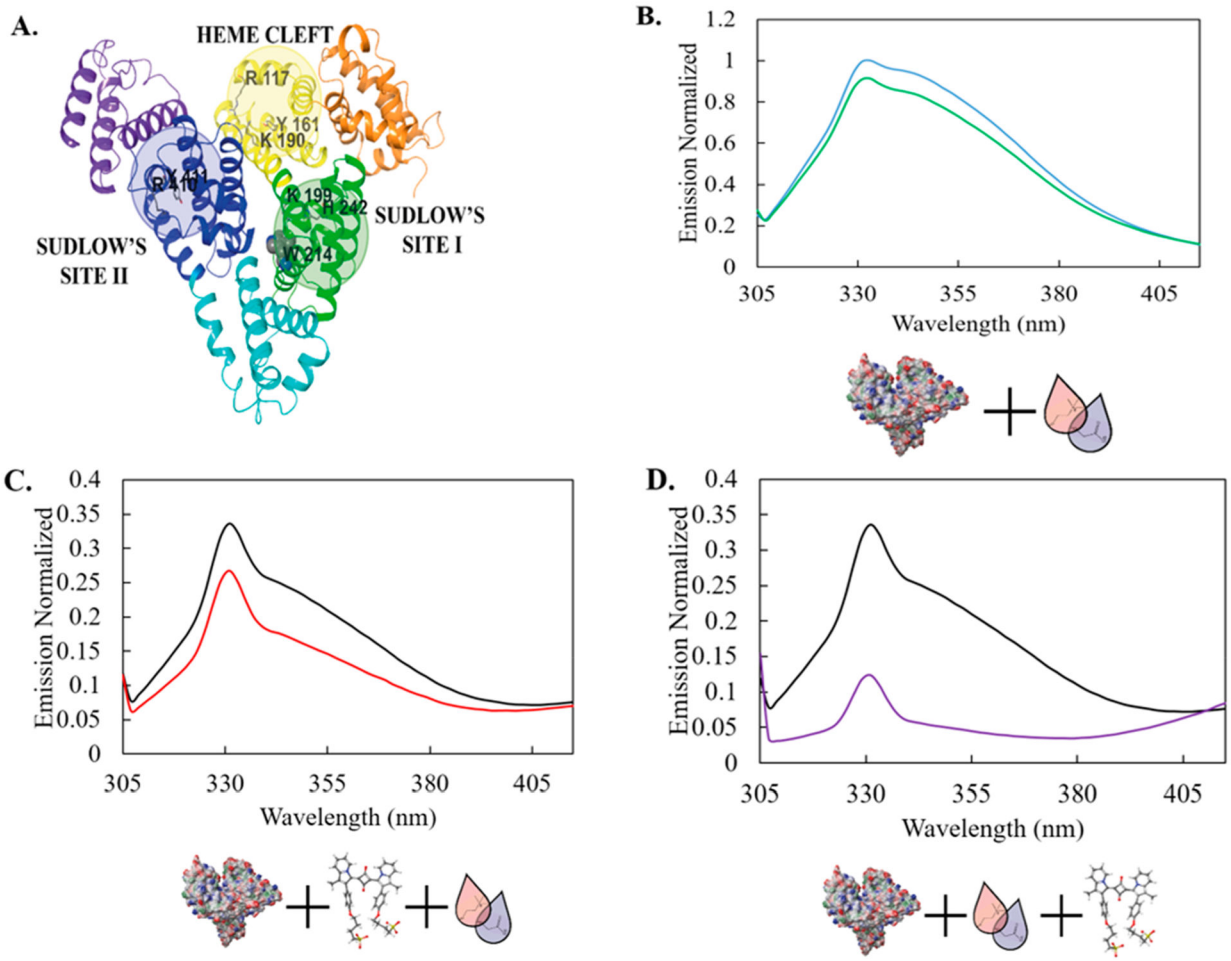

Figure 3.

The addition of SO_3SQ, CG 1:1, or a combination of the two, to a solution of HSA causes a decrease in the fluorescence of the tryptophan residue. (A) The structure of HSA with location of tryptophan residue; Fluorescence spectra of tryptophan residues under 3 conditions: (B) HSA in water (blue) with the addition of 160 mM CG (1:1) (green); (C) HSA in 10 μM SO3SQ (black) with the addition of 160 mM CG (1:1) (red); (D) HSA in solutions containing 160 mM CG (1:1) (black) prior to adding SO_3SQ (purple).

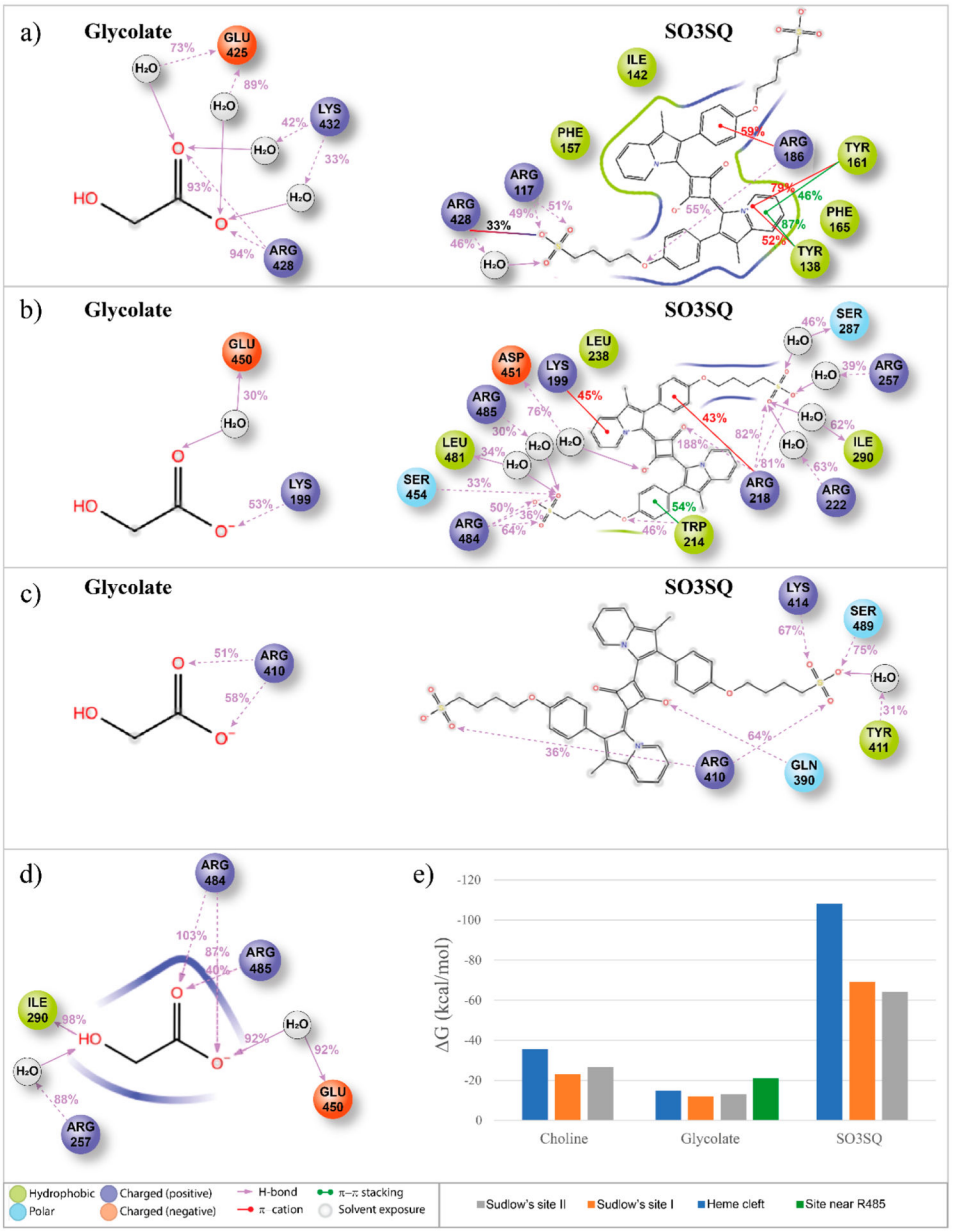

Figure 4.

The components of the IL/dye system show a greater binding affinity for the heme cleft. Results of the Molecular Dynamics simulation for complexes of SO3SQ and glycolate with HSA within (a) heme cleft, (b) Sudlow's site I, (c) Sudlow's site II, (d) site near R485, and (e) results of MM/GBSA calculation for the ligand–albumin complex after MD simulation and trajectory clustering.

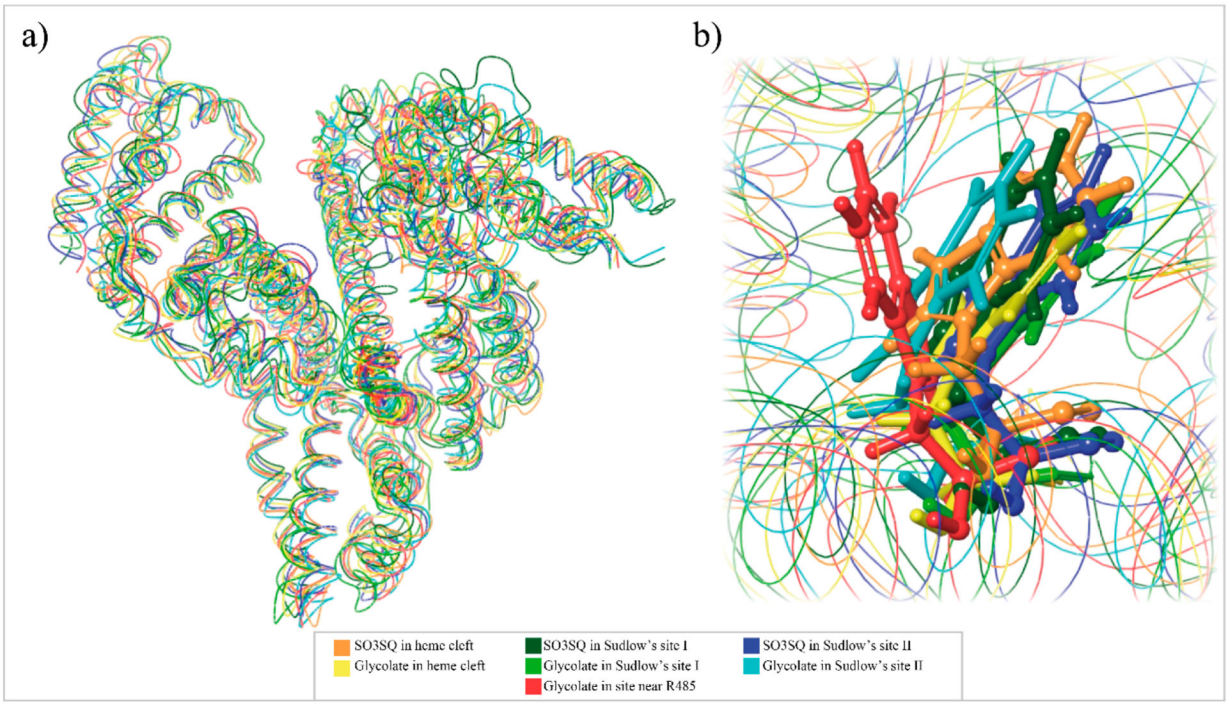

Figure 5.

Proximity of the glycolate anion to W214 results in interactions that lead to quenching of the W214 fluorescence. Superposition of ligand–protein complexes: (a) superimposed protein structures with backbone illustrated as a curved line; (b) superimposed W214 residue.

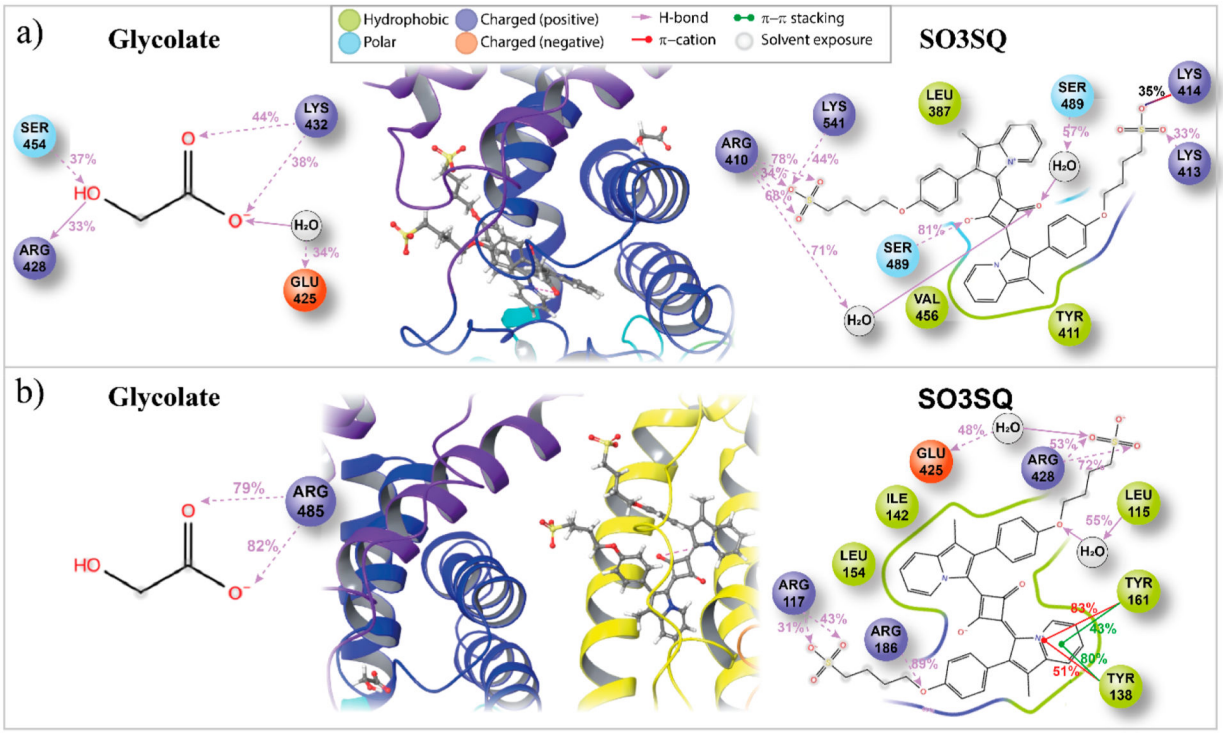

Figure 6.

The presence of 1:1 CG results in more favorable binding of SO_3SQ to the heme cleft of HSA, and slightly more improved binding in Sudlow's site II. Results of the Molecular Dynamics simulation for complexes of SO_3SQ-G-HSA with (a) glycolate in the heme cleft and SO_3SQ in Sudlow's site II and (b) glycolate in Sudlow's site II and SO_3SQ in the heme cleft.

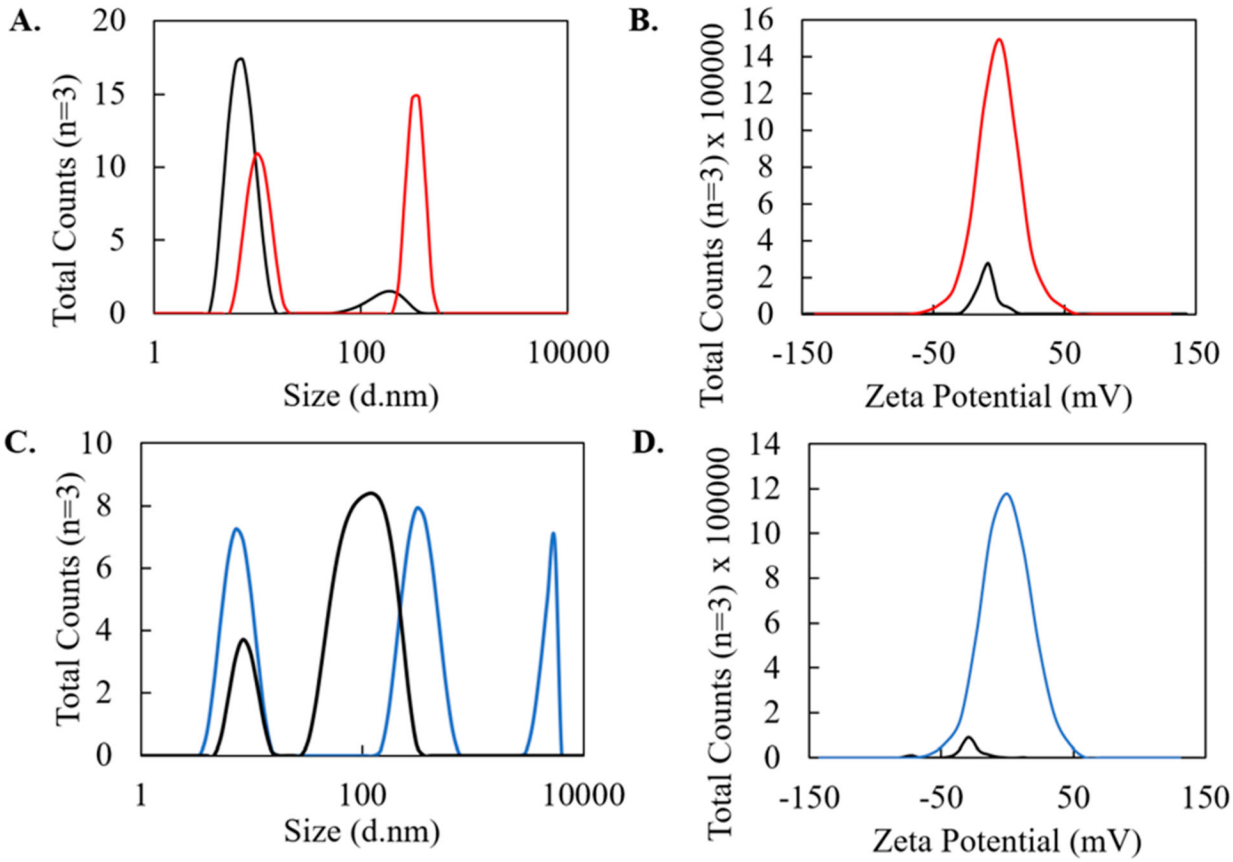

Figure 7.

Adding CG 1:1 to HSA results in a size increase and a charge that is less negative. Adding CG 1:1 to a system containing 10 μM SO3SQ and HSA causes the overall complex to increase in size and charge. Hydrodynamic diameter (intensity) of (A) HSA in water (black) and HSA in water with 160 mM CG 1:1 added (red). Zeta potential of (B) HSA in water (black), HSA in water with a 1:1 addition of 160 mM CG 1:1 added (red). Hydrodynamic diameter of (C) HSA in 10 μM SO3SQ (black), HSA in 10 μM SO3SQ with 1:1 added 160 mM CG 1:1 added (blue). Zeta potential of (D) HSA in 10 μM SO3SQ (black), HSA in 10 μM SO3SQ with a 1:1 addition of 160 mM CG 1:1 added (blue).

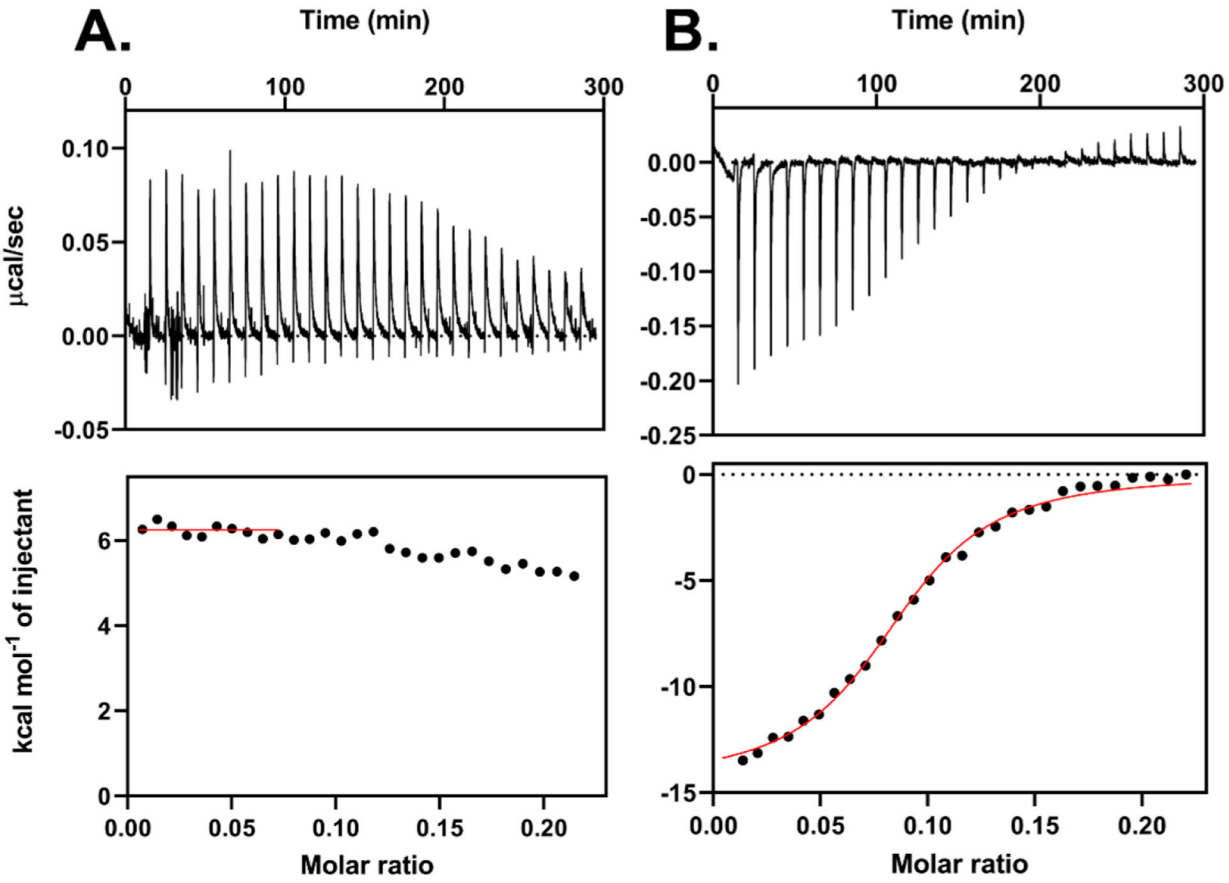

Figure 8.

The interaction between SO_3SQ and HSA is exothermic in the absence of 1:1 CG, but is endothermic in the presence of CG 1:1. Representative isothermal titration calorimetry of HSA titrations into SO_3SQ. (A) A conventional reverse titration, showing the baseline-corrected injections (top) and integrated heats (bottom) in the absence of IL. The red line indicates the best fit finding profile, which has an exothermic heat. (B) The same experiment was performed in the presence of 40 mM IL. The enthalpy becomes positive, and the complete binding profile is not observed because of solubility limitations. The red line shows the average of the first 10 injections, which was used to estimate the enthalpy of binding. Conditions are provided in the main text.

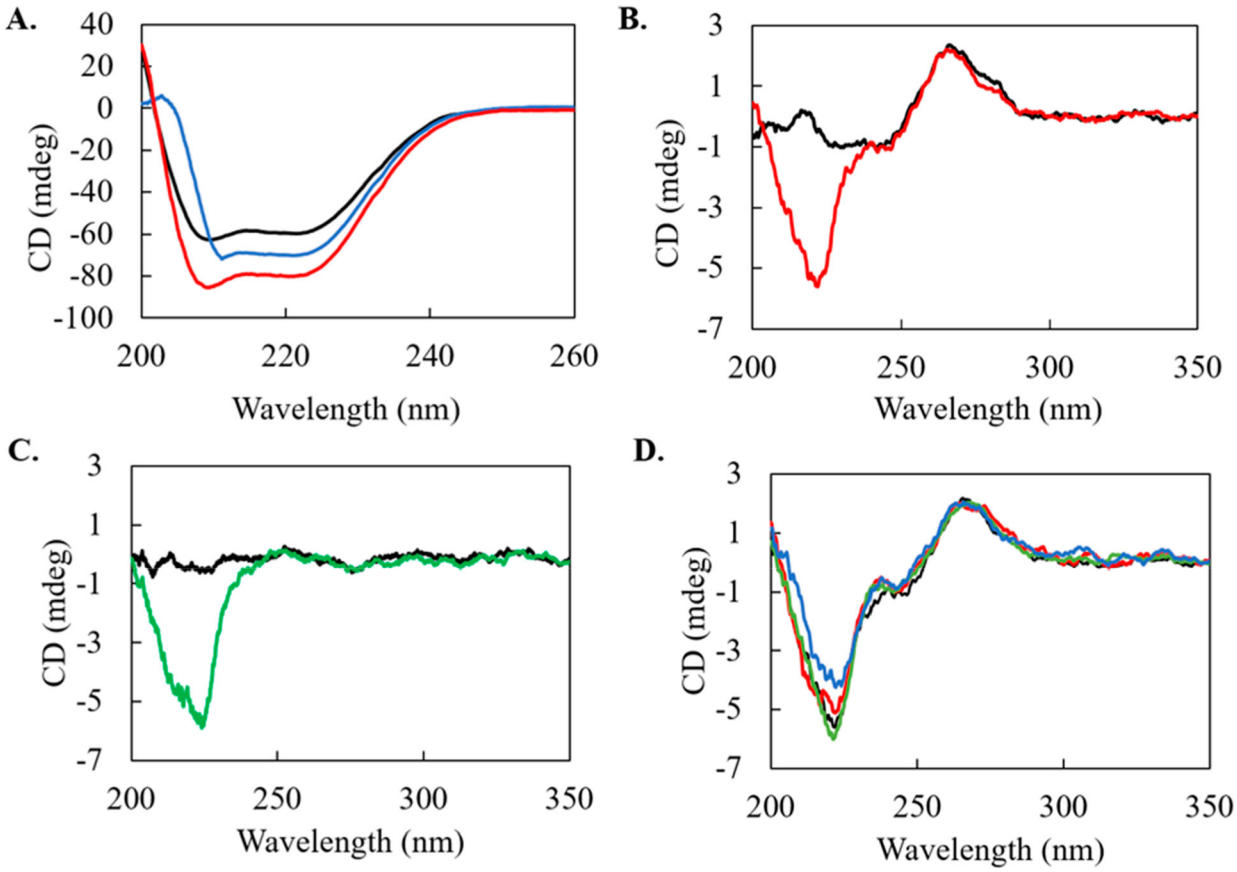

Figure 9.

The 1:1 SO_3SQ/CG system does not destroy albumin's secondary structure or compromise the integrity of DNA. CD spectra of (a) human serum albumin (HSA) (black), HSA in 10 μM dye (red), and HSA in 10 μM dye with 160 mM CG 1:1. Overlaid CD spectra of (b) DNA only (blue) and DNA in 2.5% IL (red), (c) 9.14 μM dye in water (blue) and dye in 2.5% IL (orange), (d) DNA in 2.5% IL (black), DNA in 2.5% IL with 5 μL of 1 μM dye solution (red), DNA in 2.5% IL with 10 μL of 1 μM dye solution (yellow), and DNA in 2.5% IL with 15 μL of 1 μM dye solution (blue).

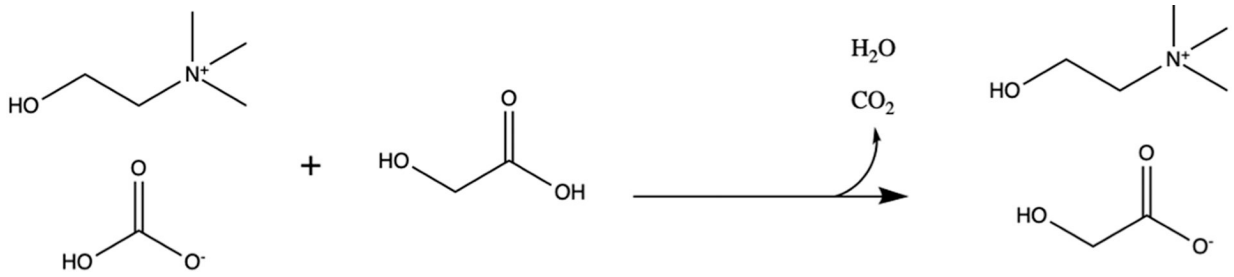

Scheme 1.

Dropwise Addition of a 1:1 Molar Ratio of Choline Bicarbonate to Glycolic Acid to Synthesize the IL Choline Glycolate (CG (1:1)) via a Salt Metathesis Reaction

Table 1.

Free Binding Energies Predicted by MM/GBSA Performed after MD Simulation and Trajectory Clustering

glycolate binds to HSA:			
condition:	**heme cleft**	**Sudlow's site I**	**Sudlow's site II**
unbound albumin	−14.78	−12.03	−13.17
Scenario 1: glycolate binds to:			
SO_3SQ is in heme cleft	−16.38	−9.75	−23.99
SO_3SQ is in Sudlow's site I	−21.94	−3.07	−13.39
SO_3SQ is in Sudlow's site II	−19.23	−4.85	−12.82
Scenario 2: SO_3SQ binds to			
glycolate is in heme cleft	−87.54	−61.26	−105.34
glycolate is in Sudlow's site I	−92.93	−68.39	−51.35
glycolate is in Sudlow's site II	−91.83	−74.59	−74.76
glycolate is near R485	−84.51	−54.78	−60.27
SO_3SQbinds to HSA:			
unbound albumin	−108.18	−69.05	−64.04